NASA TECHNICAL NOTE

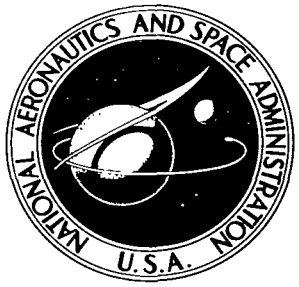

NASA TN D-2001
c. 1

LOAN COPY: RETU
AFWL (WLL-
KIRTLAND AFB, I

TECH LIBRARY KAFB, NM
0154244

NASA TN D-2001

TOUCHDOWN DYNAMICS ANALYSIS OF SPACECRAFT FOR SOFT LUNAR LANDING

by Robert E. Lavender

George C. Marshall Space Flight Center
Huntsville, Alabama

NATIONAL AERONAUTICS AND SPACE ADMINISTRATION • WASHINGTON, D. C. • JANUARY 1964

ERRATA

NASA TECHNICAL NOTE D-2001

TOUCHDOWN DYNAMICS ANALYSIS OF SPACECRAFT FOR SOFT LUNAR LANDING

By Robert E. Lavender

January 1964

Completed 15 Jul 64 ELR

Page 22: Figure 7 reads $L_1 = 285$ in., $L_2 = 326$ in. The figure is correctly read as $L_1 = 326$ in., $L_2 = 285$ in.

NASA-Langley, 1964

Issue date: 7-6-64

TECH LIBRARY KAFB, NM
0154244

TOUCHDOWN DYNAMICS ANALYSIS OF SPACECRAFT FOR SOFT LUNAR LANDING

By Robert E. Lavender

George C. Marshall Space Flight Center
Huntsville, Alabama

NATIONAL AERONAUTICS AND SPACE ADMINISTRATION

For sale by the Office of Technical Services, Department of Commerce,
Washington, D.C. 20230 -- Price $1.00

TABLE OF CONTENTS

LIST OF ILLUSTRATIONS

LIST OF ILLUSTRATIONS (CONT'D)

DEFINITION OF SYMBOLS

C	Proportionality constant between the crushing force and the stroke due to crushing during onset.
C_{10}, C_{20}	Crushing force of the uphill and downhill legs, respectively, after onset.
D	Landing gear diameter.
F	Total force acting on a foot.
F_L	Component of total force acting along the leg.
F_B	Component of total force acting normal to the leg.
F_N	Component of total force acting normal to the lunar surface.
F_T	Component of total force acting along the lunar surface.
g	Gravitational acceleration of the moon.
k	Vehicle's radius of gyration with respect to the center of gravity.
L_1	Distance from the center of gravity to the first foot measured normal to the longitudinal axis.
L_2	Original distance (before crushing) from the center of gravity to the feet measured along the longitudinal axis.
L_3	Distance from the center of gravity to the second foot measured normal to the longitudinal axis.
L. F.	Deceleration load factor based on earth gravity for landing on a level surface with all legs contacting simultaneously, $(F_{N1} + F_{N2})/W_e$.
m	Vehicle's mass.
N	Number of legs.
$\dot{S}$	Rate of sliding along the lunar surface.
T	Stabilization rocket motor thrust.

t_b	Stabilization rocket motor burning time.
Δt	Integrating time interval.
V_V	Vertical component of velocity vector, positive downward.
V_H	Horizontal component of velocity vector, positive away from hill.
V_N	Velocity normal to the lunar surface, $-\dot{y}$.
V_T	Velocity parallel to the lunar surface, $\dot{x}$.
W	Weight of vehicle at the moon, mg.
W_e	Earth weight of the vehicle landed on the moon.
x	Center of gravity coordinate along the lunar surface.
y	Center of gravity coordinate normal to the lunar surface.
α	Angle between the vertical and the line from the center of gravity to the foot.
β	Angle between the total force and the component of total force along the leg.
δ	The stroke parallel to the longitudinal axis due to crushing.
δ_{10}, δ_{20}	Designed onset stroke, or stroke during buildup of the crushing force to the maximum value, for the first and second legs, respectively (unless otherwise noted, this onset stroke has been assumed zero).
φ, $\dot{\varphi}$	Vehicle attitude and attitude rate, positive counterclockwise.
θ	Slope of lunar surface from the horizontal, positive counterclockwise.
μ	Angle between the total force and the component of total force normal to the lunar surface.
μ_o	Limiting value of μ, or angle of friction.
$\tan \mu_o$	Coefficient of friction.

$(\alpha_2)\dot{\varphi} = 0$	Dynamic stability margin; the value of α_2 at the instant the vehicle's rotation changes from negative to positive.

Subscripts:

1	First leg.
2	Second leg.
pm	Previous maximum.
(n - 1)	Value at previous time step.

NATIONAL AERONAUTICS AND SPACE ADMINISTRATION

TECHNICAL NOTE D - 2001

TOUCHDOWN DYNAMICS ANALYSIS OF SPACECRAFT FOR SOFT LUNAR LANDING

By

Robert E. Lavender

SUMMARY

Results of analytical touchdown dynamics investigations are presented which were conducted to obtain the influence of various lunar and configuration design parameters on the touchdown dynamic stability of spacecraft for use in soft landing payloads on the moon. Parameters used in the analysis include the local lunar slope, coefficient of friction, initial touchdown vertical and horizontal velocity components, vehicle weight and radius of gyration, height of the center of gravity, displacement of the center of gravity from the vehicle's longitudinal axis, thrust of stabilization rocket motors, crushing force of energy absorbing material in the leg struts, and number of legs.

Results show that the lunar slope, which was varied up to 40 degrees, and the coefficient of friction have a large effect on the landing gear diameter required for touchdown stability. The initial touchdown vertical and horizontal velocity components also have a large influence on the required landing gear diameter. Variations in the height of the center of gravity, displacement of the center of gravity from the vehicle's longitudinal axis, vehicle weight and radius of gyration, and crushing force of the energy absorbing material have less influence on the landing gear design.

The use of a stabilization rocket motor is highly effective in providing adequate touchdown dynamic stability. Significant reduction in landing gear diameter can be realized with the use of such a motor. With a properly chosen scheme for providing motor ignition, tumbling of the vehicle under severe conditions of lunar slope and friction can be prevented with a motor of relatively low total impulse. High thrust for a short burning time is required with the thrust level on the order of the configuration's earth weight.

INTRODUCTION

In the overall considerations of the design and performance of space vehicle systems intended to soft land payloads on the moon, analysis of touchdown dynamic motion of the landing stage is an important part. It would indeed be a pity for the vehicle system to perform successfully all phases of flight to the moon only to result in a failure during the few seconds of motion remaining after initial touchdown. Equations have been derived for two-dimensional touchdown dynamic analysis including crushing of energy absorbing material in the legs and sliding of the foot pads along the lunar surface.

Vehicles with legs are assumed in order to provide sufficient moment arm for the restoring forces necessary to prevent tumbling. A column of aluminum honeycomb material is assumed located within each leg which absorbs energy with essentially a constant load-stroke relationship and without rebound (Refs. 1 and 2). While other methods of energy absorption may be more efficient on a ft-lb/lb basis such as a collapsible shell (Ref. 3) or frangible tube (Ref. 4), they may be more difficult to apply to an actual landing gear designed for simple, reliable operation. Various methods of obtaining energy dissipation are considered in References 5 to 10.

The author is indebted to Mr. John D. Capps, Computation Division, who programmed the equations for the GE 225 digital computer and supported the computation of numerical results.

MATHEMATICAL MODEL

Equations for the analysis were developed corresponding to the two-dimensional touchdown dynamics model shown in Figure 1. This model is adequate for the analysis of either three - or four legged vehicles. Inelastic, crushable material to absorb energy during touchdown is assumed located within the legs. Additional energy is absorbed as a result of sliding action of the feet along the lunar surface. Motion takes place in a plane such that two legs contact the surface simultaneously for the four-legged vehicle. For the three-legged vehicle, either the double leg or single leg can initially touchdown. It is assumed that the vehicle has feet of sufficient area to prevent penetration of the lunar surface. If the bearing strength of the lunar surface is determined later to be quite low for considerable depth, then large pontoons rather than foot pads must be attached to the legs if burying the vehicle is to be avoided.

From Newton's second law, the equations of motion are

$$m\ddot{y} = F_{N1} + F_{N2} - W \cos \theta - (T_1 + T_2) \cos (\varphi - \theta) \qquad (1)$$

$$m\ddot{x} = F_{T1} + F_{T2} - W \sin\theta + (T_1 + T_2) \sin(\varphi - \theta) \tag{2}$$

$$mk^2\ddot{\varphi} = (F_{T1} + F_{T2})\, y + F_{N2}\, x_3 - F_{N1} x_1 + T_1 L_1' - T_2 L_3'. \tag{3}$$

The accelerations obtained from the above equations are integrated numerically with the use of a digital computer.

The force along the first leg is obtained by

$$F_{L1} = 0 \qquad \delta_1 < 0 \tag{4}$$

$$F_{L1} = 0 \qquad \delta_1 \geq 0\,,\ \delta_1 < \delta_{1\,pm} \tag{5}$$

$$F_{L1} = C_1 \delta_1 \qquad \delta_{1\,pm} \leq \delta_1 < \delta_{10}\,,\ \dot{\delta}_1 > 0 \tag{6}$$

$$F_{L1} = C_{10} \qquad \delta_{1\,pm} \leq \delta_1 \geq \delta_{10}\,,\ \dot{\delta}_1 > 0 \tag{7}$$

Equation (4) expresses the fact that the force along the leg is zero if the leg has not yet reached the surface, and Equation (5) the fact that the leg has previously been crushed but is now off the surface. If the leg is crushing but the length crushed is less than the designed onset length, then the crushing force is assumed proportional to the length crushed as given by Equation (6). The crushing force buildup during onset can be obtained from a column of honeycomb material, for example, by forming a wedge at one end. Equation (7) represents the crushing force after onset as a constant force characteristic of honeycomb material. The force along the second leg is determined in the same manner. These equations determine the force along the leg except when the crushing has stopped and the vehicle rotates as a rigid body. During such a rotation, the force along the leg is less than the crushing force and is obtained in a manner described later.

The length crushed and crushing rate for the legs are obtained by

$$\delta_1 = L_2 + L_1 \tan(\varphi - \theta) - y \sec(\varphi - \theta) \tag{8}$$

$$\delta_2 = L_2 - L_3 \tan(\varphi - \theta) - y \sec(\varphi - \theta) \tag{9}$$

$$\dot{\delta}_1 = -\sec^2(\varphi - \theta)\left\{ \dot{y} \cos(\varphi - \theta) + [y \sin(\varphi - \theta) - L_1]\, \dot{\varphi} \right\} \tag{10}$$

$$\dot{\delta}_2 = -\sec^2(\varphi - \theta)\left\{ \dot{y} \cos(\varphi - \theta) + [y \sin(\varphi - \theta) + L_3]\, \dot{\varphi} \right\}. \tag{11}$$

As long as a leg is crushing and also the foot is sliding along the surface, the tangential and normal forces are readily computed. The sliding rate along the surface is given by:

$$\dot{S}_i = \dot{x} + y\dot{\varphi} - \dot{\delta}_i \sin(\varphi - \theta), \tag{12}$$

where the subscript "i" is 1 or 2 for the first or second leg, respectively. Then:

$$\mu_i = -\mu_0 \frac{\dot{S}_i}{|\dot{S}_i|}, \quad \dot{S}_i \neq 0. \tag{13}$$

$$\beta_i = \varphi - \theta + \mu_i . \tag{14}$$

$$F_i = F_{Li} \sec \beta_i . \tag{15}$$

$$F_{Ni} = F_i \cos \mu_i . \tag{16}$$

$$F_{Ti} = F_i \sin \mu_i . \tag{17}$$

Thus the normal and tangential forces are determined, as long as crushing and sliding are present, and the accelerations can be obtained from the equations of motion.

Stabilization rockets can be considered in the analysis and are represented by:

$$T_1 = K_1 \qquad \delta_2 < 0, \quad t < t_{1b} \tag{18}$$

$$T_1 = 0 \qquad \delta_2 < 0, \quad t \geq t_{1b} \tag{19}$$

$$T_1 = K_{10} \qquad \delta_2 \geq 0 \tag{20}$$

$$T_2 = K_2 \qquad \delta_2 < 0, \quad t < t_{2b} \tag{21}$$

$$T_2 = 0 \qquad \delta_2 < 0, \quad t \geq t_{2b} . \tag{22}$$

This representation provides sufficient flexibility to account for a number of rocket stabilization schemes.

Whenever the sliding rate as obtained from Equation (12) changes sign, interpolation is made to determine the time at which the foot stops sliding. Once a foot stops sliding, it remains at rest unless the computed angle , μ, exceeds the angle of friction. During the time that a foot is at rest, with the leg still crushing, the normal and tangential forces are determined by an iterative procedure. The normal and tangential forces are first obtained by Equations (16) and (17) for various assumed values of μ. Equations (2) and (3) are then solved for $\ddot{x}$ and $\ddot{\varphi}$ corresponding to each value of μ assumed. Now from equation (12), with a foot at rest,

$$\dot{x} = -y\dot{\varphi} + \dot{\delta}_i \sin(\varphi - \theta) \tag{23}$$

and, by differentiating,

$$\ddot{x} = -y\ddot{\varphi} - \dot{y}\dot{\varphi} + \dot{\delta}_i \dot{\varphi} \cos(\varphi - \theta) + \ddot{\delta}_i \sin(\varphi - \theta), \tag{24}$$

where $\ddot{\delta}_i$ may be taken as

$$\ddot{\delta}_i = \frac{\dot{\delta}_i - \dot{\delta}_{i\,(n-1)}}{\Delta t} . \tag{25}$$

Thus the value of μ is determined by iteration such that $\ddot{x}$ and $\ddot{\varphi}$ obtained from Equations (2) and (3) satisfy Equation (24). Once the μ has been determined, its absolute value must be compared with the angle of friction. If it exceeds the angle of friction, μ is taken to be

$$\mu = \frac{\mu^*}{|\mu^*|} \mu_0 , \tag{26}$$

where μ^* is the value determined by the iteration. In this case the foot has started to slide again. The normal and tangential forces are determined from Equations (16) and (17) by using the μ from Equation (26), and the accelerations are obtained from Equations (1), (2), and (3). At subsequent time intervals, μ is computed by Equation (13) as long as sliding continues.

As the first leg crushes, the crushing rate determined by Equation (10) is positive. When the crushing rate changes from positive to negative, the time at which the crushing stops is determined by interpolation, and the force along the leg can no longer be determined by Equations (6) or (7). The vehicle may then rotate as a rigid body about the first foot. Sliding of the first foot may or may not be present. From Figure 1,

$$y = (L_2 - \delta_1) \cos(\varphi - \theta) + L_1 \sin(\varphi - \theta) , \tag{27}$$

and, when the crushing rate is zero,

$$\dot{y} = -(L_2 - \delta_1) \dot{\varphi} \sin(\varphi - \theta) + L_1 \dot{\varphi} \cos(\varphi - \theta). \tag{28}$$

But from Figure 1,

$$x_1 = L_1 \cos(\varphi - \theta) - (L_2 - \delta_1) \sin(\varphi - \theta), \tag{29}$$

so that

$$\dot{y} = x_1 \dot{\varphi} \tag{30}$$

and

$$\ddot{y} = x_1 \ddot{\varphi} - y \dot{\varphi}^2 . \tag{31}$$

If sliding is present, the value of μ_1 is known from equation (13) and the normal and tangential forces are

$$F_{N1} = F_{L1} \sec \beta_1 \cos \mu_1 \tag{32}$$

$$F_{T1} = F_{L1} \sec \beta_1 \sin \mu_1 . \tag{33}$$

Substitution of Equations (31), (32), and (33) into Equations (1) and (3) results in two equations from which the unknowns $\ddot{\varphi}$ and F_{L1} may be obtained:

$$m x_1 \ddot{\varphi} - F_{L1} \sec \beta_1 \cos \mu_1 = F_{N2} - W \cos \theta + m y \dot{\varphi}^2 - (T_1 + T_2) \cos (\varphi - \theta) \tag{34}$$

$$m k^2 \ddot{\varphi} + [\sec \beta_1 (x_1 \cos \mu_1 - y \sin \mu_1)] F_{L1} = F_{T2} y + F_{N2} x_3 + T_1 L_1' - T_2 L_3' . \tag{35}$$

If the value of F_{L1} obtained is positive, the vehicle rotates as a rigid body about the first foot (with sliding present) and the proper forces and accelerations are determined. However, if this value is negative, the first foot is off the surface, and the forces are set equal to zero. The values of $\ddot{\varphi}$ and F_{L1} obtained from Equations (34) and (35) are therefore not valid. Equations (1), (2), and (3) are then solved for the accelerations with the forces on the first foot set to zero. If the second foot has not yet reached the surface, the vehicle is thus in free flight.

If sliding is not present, then the value of μ_1 is not known from Equation (13) and must be obtained in another manner. For this case the vehicle is in pure rotation about the first foot without sliding or crushing. In such a case,

$$\ddot{x} = \ddot{x}_1 . \tag{36}$$

Differentiating Equation (29) with the crushing rate zero,

$$\dot{x}_1 = - y \dot{\varphi} \tag{37}$$

and

$$\ddot{x}_1 = - y \ddot{\varphi} - x_1 \dot{\varphi}^2 . \tag{38}$$

Substitution of Equations (31) and (38) into Equations (1), (2), and (3) yields three equations from which the three unknowns $\ddot{\varphi}$, F_{T1}, and F_{N1} may be obtained:

$$F_{N1} - m x_1 \ddot{\varphi} = - F_{N2} - m y \dot{\varphi}^2 + W \cos \theta + (T_1 + T_2) \cos (\varphi - \theta). \tag{39}$$

$$F_{T1} + m y \ddot{\varphi} = - F_{T2} - m x_1 \dot{\varphi}^2 + W \sin \theta - (T_1 + T_2) \sin (\varphi - \theta). \tag{40}$$

$$x_1 F_{N1} - y F_{T1} + m k^2 \ddot{\varphi} = y F_{T2} + x_3 F_{N2} + T_1 L_1' - T_2 L_3' \tag{41}$$

If the value of F_{N1} obtained is positive, the vehicle rotates about the first foot. The value for μ_1 is

$$\mu_1 = \tan^{-1} \frac{F_{T1}}{F_{N1}} . \tag{42}$$

If $|\mu_1| > \mu_0$, μ_1 is set equal to μ_0 with the sign of μ_1 the same as given from Equation (42). The foot has thus started to slide, and the values obtained from Equations (39), (40), and (41) are not valid. However, since μ_1 is now known, the proper forces and accelerations are determined using Equations (34) and (35). If the value of F_{N1} obtained is negative, the foot is off the surface and the forces are set equal to zero.

After the second leg contacts the surface, the sliding may stop before the leg stops crushing. In this case, F_{L2} is known, and μ_2 is determined by the iterative procedure previously described. If the second leg stops crushing and the foot is still sliding, μ_2 is known and F_{L2} is obtained (along with $\ddot{\varphi}$) from the solution of two equations similar to Equations (34) and (35). In this case,

$$- m x_3 \ddot{\varphi} - F_{L2} \sec \beta_2 \cos \mu_2 = F_{N1} - W \cos \theta + m y \dot{\varphi}^2 - (T_1 + T_2) \cos (\varphi - \theta) \tag{43}$$

$$m k^2 \ddot{\varphi} - [\sec \beta_2 (x_3 \cos \mu_2 + y \sin \mu_2)] F_{L2} = y F_{T1} - x_1 F_{N1} + T_1 L_1' - T_2 L_3' , \tag{44}$$

where

$$x_3 = (L_2 - \delta_2) \sin (\varphi - \theta) + L_3 \cos (\varphi - \theta). \tag{45}$$

Once F_{L2} is obtained, the normal and tangential forces follow from Equations (16) and (17). Equations (1) and (2) provide the other accelerations required.

When the second leg is not crushing and the foot is not sliding, three equations are required from which $\ddot{\varphi}$, F_{T2}, and F_{N2} are obtained:

$$F_{N2} + m x_3 \ddot{\varphi} = - F_{N1} - m y \dot{\varphi}^2 + W \cos\theta + (T_1 + T_2) \cos (\varphi - \theta). \tag{46}$$

$$F_{T2} + m y \ddot{\varphi} = - F_{T1} + m x_3 \dot{\varphi}^2 + W \sin \theta - (T_1 + T_2) \sin (\varphi - \theta). \tag{47}$$

$$- x_3 F_{N2} - y F_{T2} + m k^2 \ddot{\varphi} = y F_{T1} - x_1 F_{N1} + T_1 L_1' - T_2 L_3' . \tag{48}$$

The foot remains at rest as long as $|\mu_2|$ does not exceed the angle of friction.

From Figure 1, it is seen that the vehicle tumbles about the first leg if the angle, α_1, becomes negative; it tumbles about the second leg if the angle α_2, becomes negative. These angles are given by

$$\alpha_1 = \tan^{-1} \left(\frac{x_1}{y}\right) - \theta \tag{49}$$

$$\alpha_2 = \tan^{-1} \left(\frac{x_3}{y}\right) + \theta. \tag{50}$$

RESULTS AND DISCUSSION

The equations developed have been used to obtain touchdown dynamic results for spacecraft of a size compatible with delivery of logistic supplies to the moon using a Saturn V class launch vehicle. An example is shown in Figure 2 illustrating the manner in which the landing gear spread required for stable performance is determined. For a given set of conditions, runs are made for a series of landing gear spreads. If the spread is too small, the vehicle tumbles and the rate of rotation is noted as the angle, α_2, passes through zero. If the spread is larger than necessary, the vehicle's rotational rate changes sign as the vehicle's motion becomes stable. The magnitude of the angle, α_2, as the rotational rate goes through zero is a measure of the dynamic stability margin. The required landing gear spread is determined by the intersection of the rotation rate ($\dot{\varphi}$) curve and the stability margin (α_2) curve. For a four-legged vehicle, the landing gear diameter required is $2L_1$ sec 45°. Landing gear diameters determined in this manner are the minimum required with no safety margin.

The landing gear diameter required for landing on a 30-degree lunar slope is shown in Figure 3 as a function of the height to the center of gravity for several values of the coefficient of friction and radius of gyration. As expected, the landing gear diameter increases with increasing height to the center of gravity and with larger values for the coefficient of friction. Somewhat less obvious is the increased diameter required as the radius of gyration is increased. The corresponding landing gear ratio is presented in Figure 4.

The required landing gear ratio for a typical vehicle is shown as a function of lunar slope in Figure 5. The results indicate, as expected, that the lunar slope has an important effect upon the landing gear spread required for stable touchdown.

The friction coefficient appears to be one of the most important parameters which determine the landing gear spread required to achieve touchdown stability. As seen from Figure 6, the landing gear ratio increases rapidly with increasing friction up to a coefficient of friction of about 1.0 and then levels off to an almost constant value. Since a friction coefficient of 0.577 or larger is required merely to hold a vehicle initially at rest on a 30-degree slope, the portion of the curve below this value is academic, since the vehicle gains sliding velocity and sooner or later would strike a boulder at high speed. It is important to design the foot pads to provide sufficient friction to stop the vehicle if landings on such steep slopes are required.

There are two points of comparison between Figures 4 and 6 which have the same parameter values except for vehicle weight and strength of crushable material. The required landing gear ratio is the same at both these points of comparison even though the vehicle weight is different by 8,000 pounds. Thus it appears that the vehicle weight does not affect the landing gear spread required as long as the crushing strength is selected to provide a given deceleration load factor. The crushing strength was selected

based upon a 6 g (earth) load factor for the vehicle landing on a level surface with all four feet contacting simultaneously. This result is as expected since the equations of motion could be made nondimensional through division by the vehicle's lunar weight. This was not done since the printout was desired in dimensional form.

The downhill stability boundary has been determined for a typical vehicle as a function of the initial horizontal and vertical velocity components. Results are presented in Figure 7. For a given vertical velocity, the vehicle tumbles as the initial horizontal velocity is increased beyond the stability boundary. The amount of horizontal velocity that can be tolerated increases from zero as the initial vertical velocity decreases for vertical velocities below about 8 meters per second. The upper boundary is of less interest since vertical velocities of 11 to 14 meters per second would produce large strokes during crushing. However, the curve clearly shows that if the horizontal component of velocity cannot be controlled to less than 2 meters per second, for example, then the vertical velocity must be maintained to 5 meters per second or less. If this control of vertical velocity cannot be provided, then the vertical velocity must be increased to at least 13 meters per second and either a larger stroke or larger load factor accepted.

An example of the effect the horizontal and vertical velocity components have on the required landing gear diameter is shown in Figure 8. These results show the penalty which must be paid in increased landing gear size as the initial velocity components are increased. If the engines used for descent to the lunar surface can operate until the vehicle has sensed contact with the surface, then the initial touchdown velocity can be small. However, if engine cutoff is necessary before contact in order to avoid possible unfavorable interaction, the subsequent free fall will increase the initial touchdown velocity.

Another method of providing stability, instead of simply increasing the landing gear spread, is by the use of stabilization rockets. Two methods of employment of the rocket motors were investigated. One method was to locate a rocket motor at each foot. The other method consisted of mounting a single rocket motor on top of the payload directed downward through the center of gravity. This method has the advantage of requiring only one stabilization rocket motor.

For a downhill case, corresponding to an initial horizontal velocity away from the hill, the vehicle will contact the lunar surface and rotate about the uphill legs until the downhill legs contact the surface. At this point, the rocket motor is ignited which resists the subsequent rotation about the downhill legs. If rockets are mounted on each foot (directed downward), the rocket motors are ignited on the uphill legs when the downhill legs make contact. In this analysis the vehicle's attitude angle at touchdown is considered to be less than the lunar slope encountered so that the first legs to sense contact will be the uphill legs and the opposite legs are the downhill legs.

For the uphill case, corresponding to a horizontal velocity toward the hill, no rocket motor would ignite to resist the uphill rotation. However, the initial vertical

velocity acts to resist any uphill rotation so that this case is not critical.

An example of the use of a stabilization rocket is shown in Figure 9. The configuration has a landing gear diameter of 600 inches. A thrust of 46,000 pounds with a burning time of 0.5 second will stop the vehicle's tumbling motion with a stability margin of 2 degrees. Higher thrust motors of essentially constant total impulse will provide larger margins of stability. Computations were also performed for this configuration with a motor at each foot. For this case a thrust of 11,500 pounds with a burning time of 0.5 second also provides a stable touchdown with a stability margin of 2 degrees. From these results it appears that about 23,000 pound-seconds total impulse is required for this vehicle, whether it is provided with a single motor or divided into a motor at each foot.

A single motor of this size would require only about 100 pounds of propellant and a total motor weight of about 150 pounds. Since this vehicle would require a landing gear diameter of over 900 inches without the stabilization rocket, it appears that considerable savings in weight could be realized by reducing the diameter to 600 inches and employing the stabilization rocket motor.

The uphill stability has been determined for this configuration and is presented in Figure 10. Although the stabilization rocket is present, for uphill rotation the rocket does not ignite since the rocket ignition scheme is based upon downhill leg contact. As may be seen, however, the uphill case is not critical. Horizontal velocity toward the hill of about 3 meters per second can be tolerated even for no vertical velocity component.

Since a horizontal velocity toward a hill can be considered to be a tangential component of less magnitude along the hill together with a normal velocity component, it would be expected that a lunar slope of zero would be the most critical "uphill" case since the tangential velocity would be maximum and the normal velocity would be zero. As may be seen, however, the horizontal velocity which can be tolerated is still about 3 meters per second (with no vertical velocity component) when the slope is made zero. It may also be seen that an increase of the initial vehicle attitude to 5 degrees, together with an initial attitude rate of 5 degrees per second, does not seriously affect the uphill stability. The configuration, thus stable uphill, will begin rotating downhill. Tumbling downhill is prevented by the ignition of the stabilization rocket when the downhill legs make contact.

A logistic vehicle configuration with a stabilization rocket could be used for the initial flights where lunar slopes of up to 30 degrees (or perhaps greater) might be encountered. At some later time, if a more favorable landing area can be specified which has less slope, the stabilization rocket can be removed and the weight saved used for additional logistic material. This configuration corresponds to a landing gear ratio of 0.744. As seen from Figure 5, this configuration is stable without the stabilization rocket for lunar slopes of up to 10 degrees.

The effect of displacement of the vehicle's center of gravity from the longitudinal axis is shown for a typical vehicle in Figure 11. The displacement was made such that the moment arm of the uphill leg forces was increased, while the restoring moment arm decreased for the downhill legs.

The effect of load factor on the required landing gear diameter is shown in Figure 12. The original height to the center of gravity (before leg deflection) has been made a function of the load factor in order to compensate for the increased stroke with decreased load factor. The same clearance is thus provided after stroking for the configurations landing on a level surface with all legs contacting simultaneously.

For the three-leg configuration, the landing is on one uphill leg first, free flight after crushing, and then on two downhill legs. The downhill legs deflect approximately six times more than the uphill leg. For the four-leg vehicle, the landing is on two uphill legs, free flight after crushing, and then on two downhill legs. The downhill legs deflect between two and three times more than the uphill legs. The five-leg vehicle lands on one leg, goes into free flight after crushing, and then lands on the other four legs almost simultaneously. The two downhill legs deflect about three times more than the single uphill leg. Although the two middle legs are in contact with the surface only a fraction of a second, the friction forces acting upon these legs cause significant increase in the vehicle's angular rotation. The diameter required for stable touchdown is considerably larger than would be required if the middle legs did not contact the surface. The six-leg configuration lands on two legs, goes into free flight after crushing, and then lands on the other four legs almost simultaneously. Deflection of the two downhill legs is about three to four times larger than the two uphill legs. The middle legs deflect about the same as the uphill legs. Leg deflections obtained are shown in Figures 13 through 16.

Although the touchdown dynamics program was not developed for application to five- or six-legged vehicles, analysis of these vehicles was possible because of the free flight nature of part of the motion. After the uphill leg or legs impact and the vehicle goes into free flight, the run is stopped, and values are inserted which represent the middle legs for the remainder of the motion. This technique can be used as long as the uphill legs, middle legs, and downhill legs are not all in contact with the surface simultaneously.

One of the most interesting results is that the six-leg configurations require a slightly larger landing gear diameter than the five-leg configurations. This result was obtained for all the deceleration load factors considered. The reasons for this are not obvious. The six-leg vehicle initially contacts on two legs producing a larger angular acceleration than the five-leg vehicle. It also goes into free flight somewhat sooner with a slightly higher rate of rotation. However, as the middle and downhill legs contact the surface, the unstabilizing effect of the two middle legs is larger for the five-leg vehicle than for the six-leg vehicle. This is because the crushing force in each leg is larger

by a factor of 1.2 resulting in a larger force vector which also acts through a longer moment arm. As a result the rotational rate of the five-leg vehicle increases more rapidly so that the middle legs remain in contact with the surface for less time. Therefore the middle legs for the five-leg vehicle crush for a smaller stroke and absorb less energy. Thus as the middle legs leave the surface, the two downhill legs must remove the remaining energy before the vehicle tumbles. Because the middle legs of the six-leg vehicle crush for a longer stroke, the component of velocity normal to the surface (at the instant the middle legs leave the surface) is less than for the five-leg vehicle. As a result less time is needed to change the normal velocity from a value toward the surface to a value away from the surface which is compatible with rigid body rotation. Thus the downhill legs for the six-leg vehicle crush for less time and reduce the rotational rate by a smaller amount. The six-leg vehicle, therefore, begins a rigid body rotation on the two downhill legs with a slightly higher rotational rate and therefore greater tendency to tumble.

An example of how the energy is absorbed by the crushing and sliding action has been obtained for a typical vehicle. Initial and final positions of the vehicle are shown in Figure 17 for the set of parameters listed.

The vehicle first impacts on the uphill leg and begins to crush and slide. Sliding of the foot stops in about 0.01 second while crushing continues for over 0.10 second until the vehicle gains sufficient rotational rate to cause the foot to leave the surface. The vehicle remains in free flight for almost 1.0 second until the downhill legs contact the surface and begin to crush and slide. At 0.008 second after the downhill legs begin crushing, the middle legs also contact the surface. The middle legs stop sliding about 0.014 second after contact. The middle legs stop crushing and lift off the surface about 0.04 second after their initial contact. The downhill legs stop crushing about 0.175 second after their initial contact, but continue to slide for another 2.6 seconds. The vehicle then rotates as a rigid body about the downhill legs for about 0.85 second until the rotation toward tumbling stops and the vehicle is in the final position shown in Figure 17. Total time elapsed from the initial contact is about 4.7 seconds.

The initial potential energy based on the reference plane shown in Figure 17 is

$$(PE)_o = W(H_o + d \tan \theta) = 316,790 \text{ ft-lb.}$$

The initial kinetic energy is

$$(KE)_o = \frac{1}{2} m (V_V^2 + V_H^2) = 247,570 \text{ ft-lb.}$$

Final potential energy is

$$(PE)_f = WH_f = 165,310 \text{ ft-lb.}$$

and the final kinetic energy is zero as the rotation comes to a stop. The difference in initial and final energy then is 399,050 ft-lb and should equal the work done by sliding and crushing. While the crushing force during crushing is constant in this analysis so that the work done during crushing is simply the crushing force times the stroke, the work done during sliding is computed by

$$W_S = \int F_T \dot{S} \, dt.$$

The work done during crushing and sliding for the example considered is listed below:

	Work ft-lb	Per cent of Total
Uphill Leg Crushing	46,360	11.5
Middle Legs Crushing	12,640	3.1
Downhill Legs Crushing	279,520	69.4
Uphill Foot Sliding	650	0.2
Middle Legs Sliding	5,800	1.4
Downhill Legs Sliding	57,930	14.4
Total	402,900	100.0

The work done thus agrees with the difference between initial and final energy to within one per cent.

CONCLUDING REMARKS

A lunar logistic vehicle capable of stable touchdown on lunar slopes of up to 30 degrees with a high coefficient of friction will require a relatively large landing gear diameter. Reduction of either the lunar slope or coefficient of friction significantly reduces the landing gear diameter required for stability. Reduction of lunar slope from 30 degrees to 10 degrees has been shown to decrease the landing gear ratio required by 0.4 corresponding to a reduction in landing gear diameter of about 300 inches. Reduction of the coefficient of friction from 1.00 to 0.60 results in a similar significant reduction of the required landing gear diameter.

The use of a stabilization rocket motor mounted on top of the payload and directed downward through the vehicle's center of gravity is very effective in obtaining touchdown stability under severe conditions of lunar slope and friction. Such a motor significantly reduces the landing gear diameter required. A motor with a total impulse of only 23,000 pound-seconds can reduce the required landing gear diameter by over 300 inches.

The initial vertical and horizontal components of velocity have a strong effect on the landing gear diameter required. Increase of either velocity component by one

meter per second can increase the required landing gear diameter by 30 to 50 inches.

Variations in the height of the center of gravity result in about 30 inches increase in the landing gear diameter for 10 inches increase in height of center of gravity. A displacement of 10 inches of the center of gravity from the longitudinal axis requires about 20 inches increase in the landing gear diameter. A change of the radius of gyration from 7 feet to 9 feet requires about 10 to 25 inches increase in landing gear diameter.

The landing gear diameter required for the three-legged vehicle is considerably larger than for the four-legged configuration. Some additional reduction in gear diameter is achieved with the use of five legs, but the six-legged vehicle requires a slightly larger landing gear than the five-legged vehicle.

With an increase in the initial height to the center of gravity for a decrease in the designed load factor, the required landing gear diameter increases with decreasing load factor. Thus, based on the same clearance between the vehicle and lunar surface after stroking, the landing gear diameter is increased with decreasing load factor.

REFERENCES

1. Anon., Energy Absorption Properties of Aluminum Honeycomb. TSB-110, Hexcel Products, Inc., Jan. 10, 1960.

2. Lewallen, J. Mayne, and E. A. Ripperger, Energy - Dissipating Characteristics of Trussgrid Aluminum Honeycomb. SMRL RM-5, Structural Mech. Res. Lab., Univ. of Texas, March 1962.

3. Coppa, Anthony P., Collapsible Shell Structures for Lunar Landing. Preprint No. 2156-61, Am. Rocket Soc., Inc., Oct. 1961.

4. McGehee, John R., A Preliminary Experimental Investigation of An Energy - Absorption Process Employing Frangible Metal Tubing. NASA TN D-1477, 1962.

5. Esgar, Jack B., and William C. Morgan, Analytical Study of Soft Landings on Gas-Filled Bags. NASA TR R-75, 1960.

6. Fisher, Lloyd J., Jr., Landing Energy Dissipation for Manned Reentry Vehicles. NASA TN D-453, 1960.

7. Levings, Nelson T., Jr., Launching and Alightment Systems for Aerospace Vehicles. TR 60-857, WADD, May 1961.

8. Fisher, Lloyd J., Jr., Landing Impact Dissipation Systems. NASA TN D-975, 1961.

9. McGehee, John R., and Victor L. Vaughan, Jr., Model Investigation of the Landing Characteristics of a Reentry Spacecraft with a Vertical - Cylinder Air Bag for Load Alleviation. NASA TN D-1027, 1962.

10. Esgar, Jack B., Survey of Energy - Absorption Devices for Soft Landing of Space Vehicles. NASA TN D-1308, 1962.

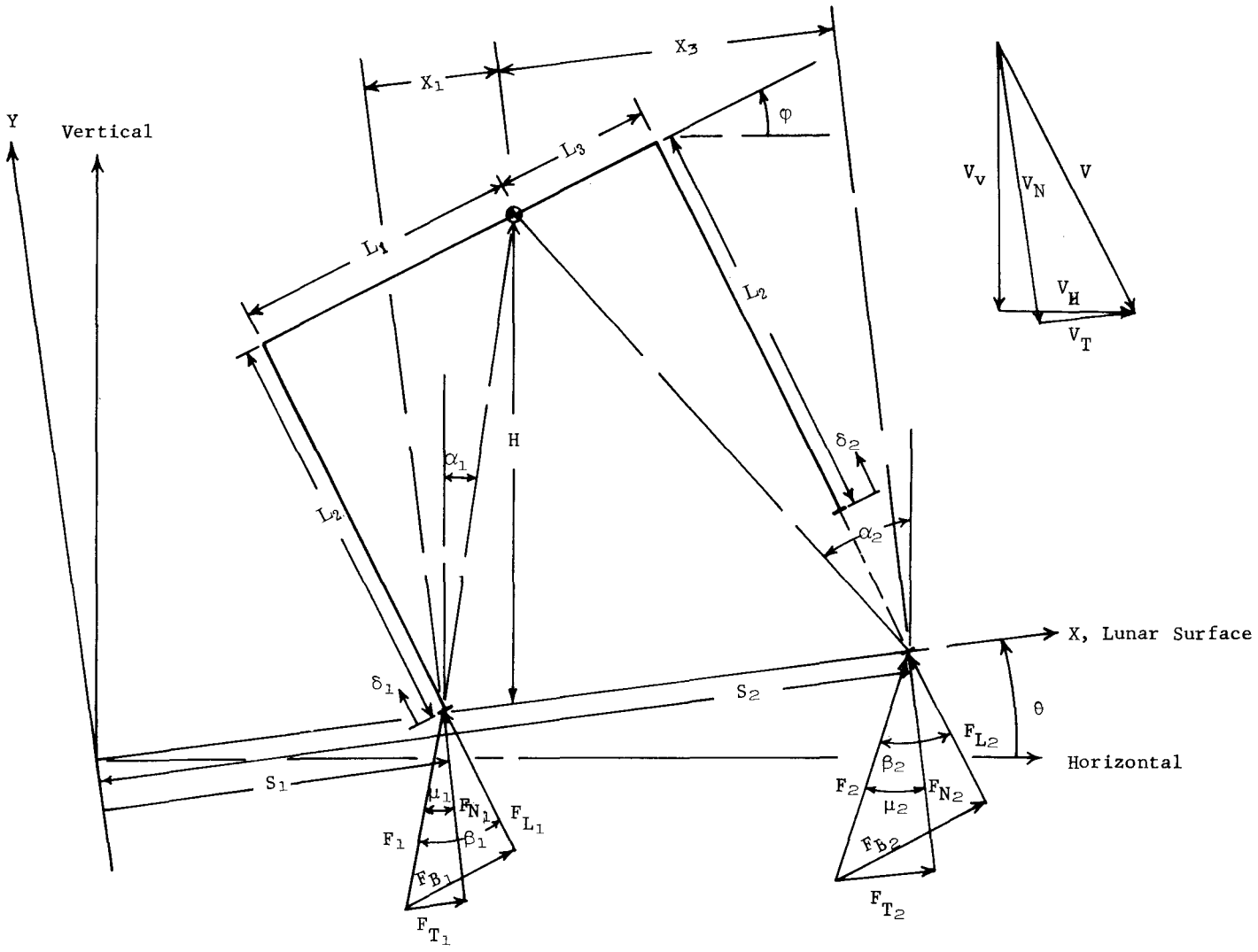

FIGURE 1. TWO-DIMENSIONAL TOUCHDOWN DYNAMICS MODEL

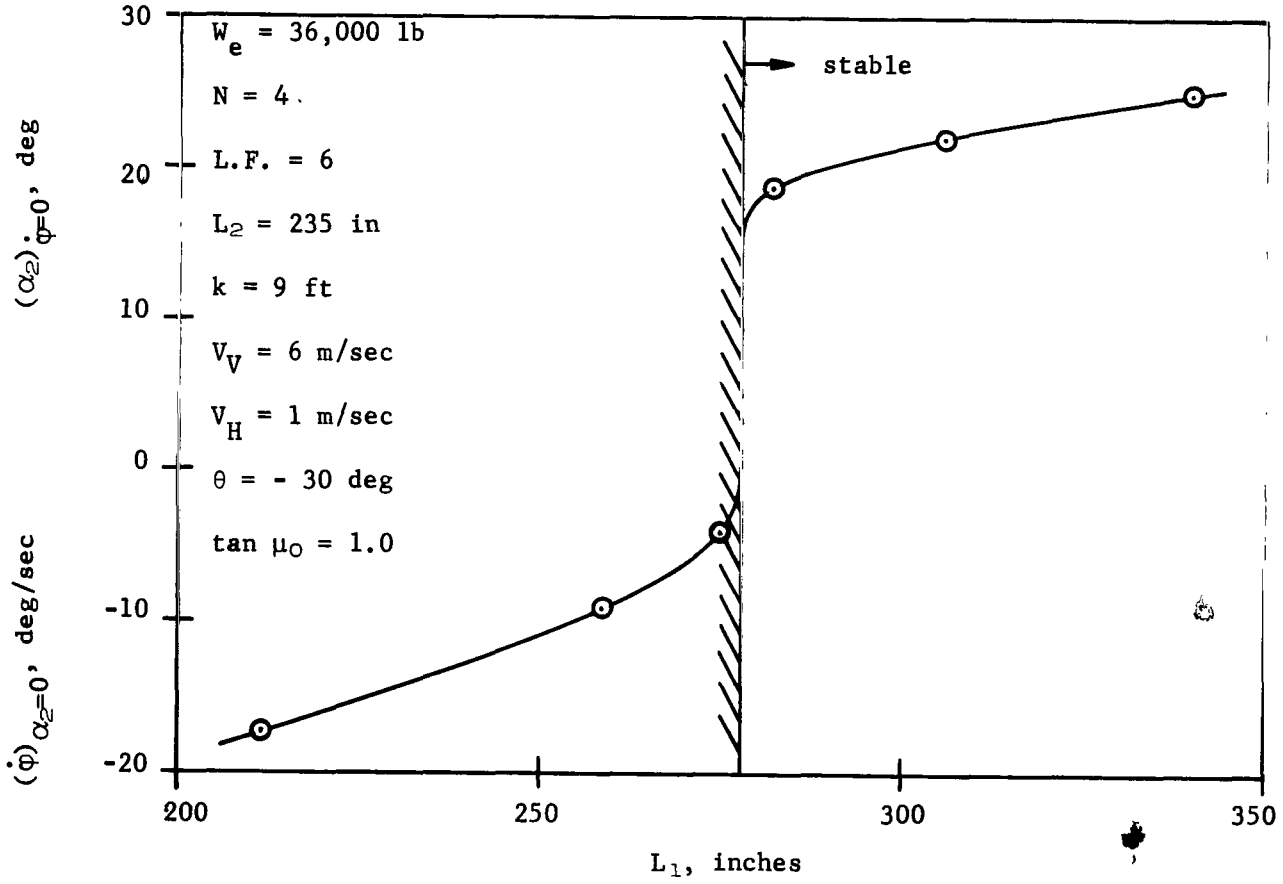

FIGURE 2. TOUCHDOWN DYNAMICS RESULTS AS A FUNCTION OF LANDING GEAR SPREAD

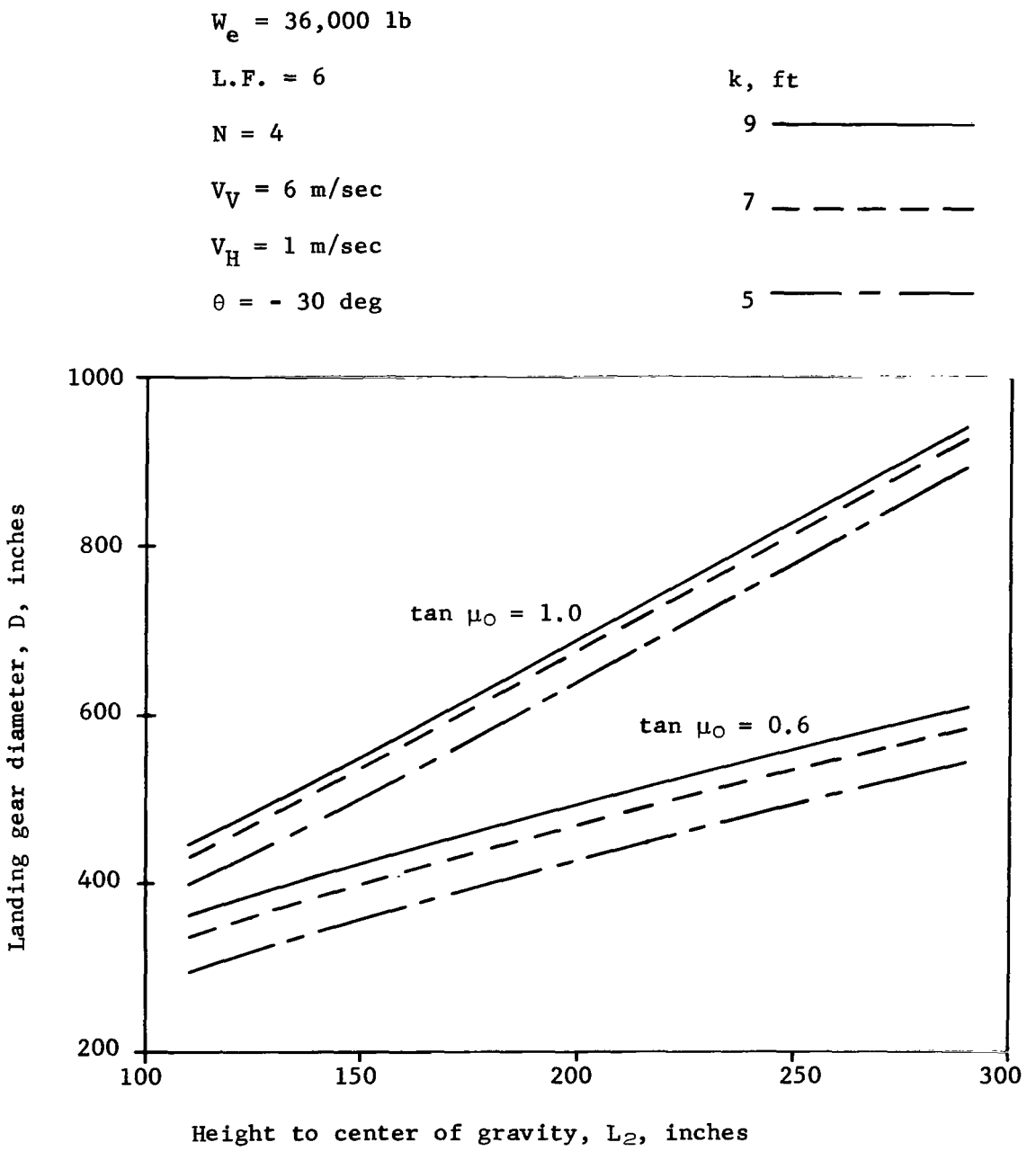

FIGURE 3. LANDING GEAR DIAMETER REQUIRED FOR STABLE TOUCHDOWN

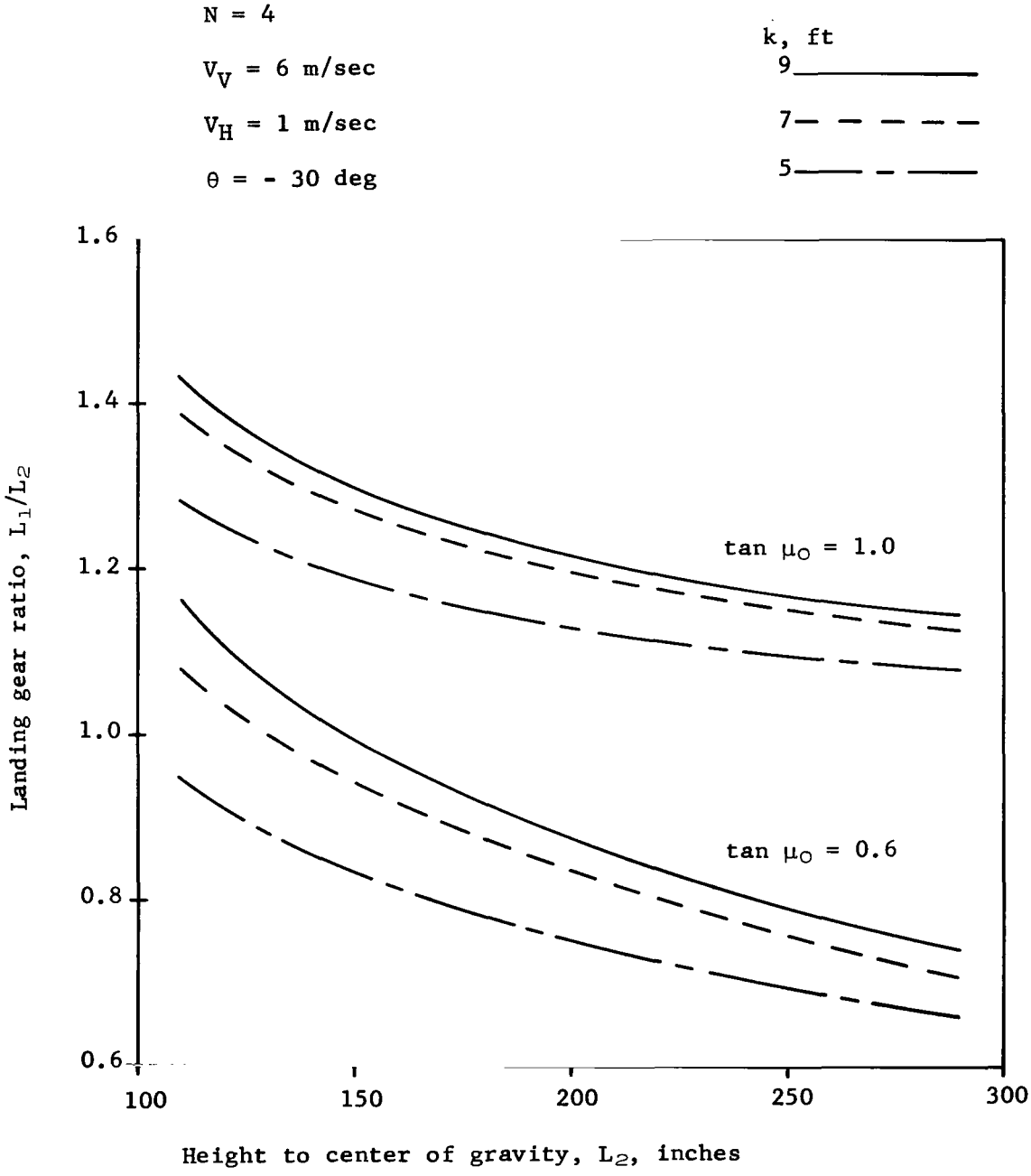

FIGURE 4. LANDING GEAR RATIO REQUIRED FOR STABLE TOUCHDOWN

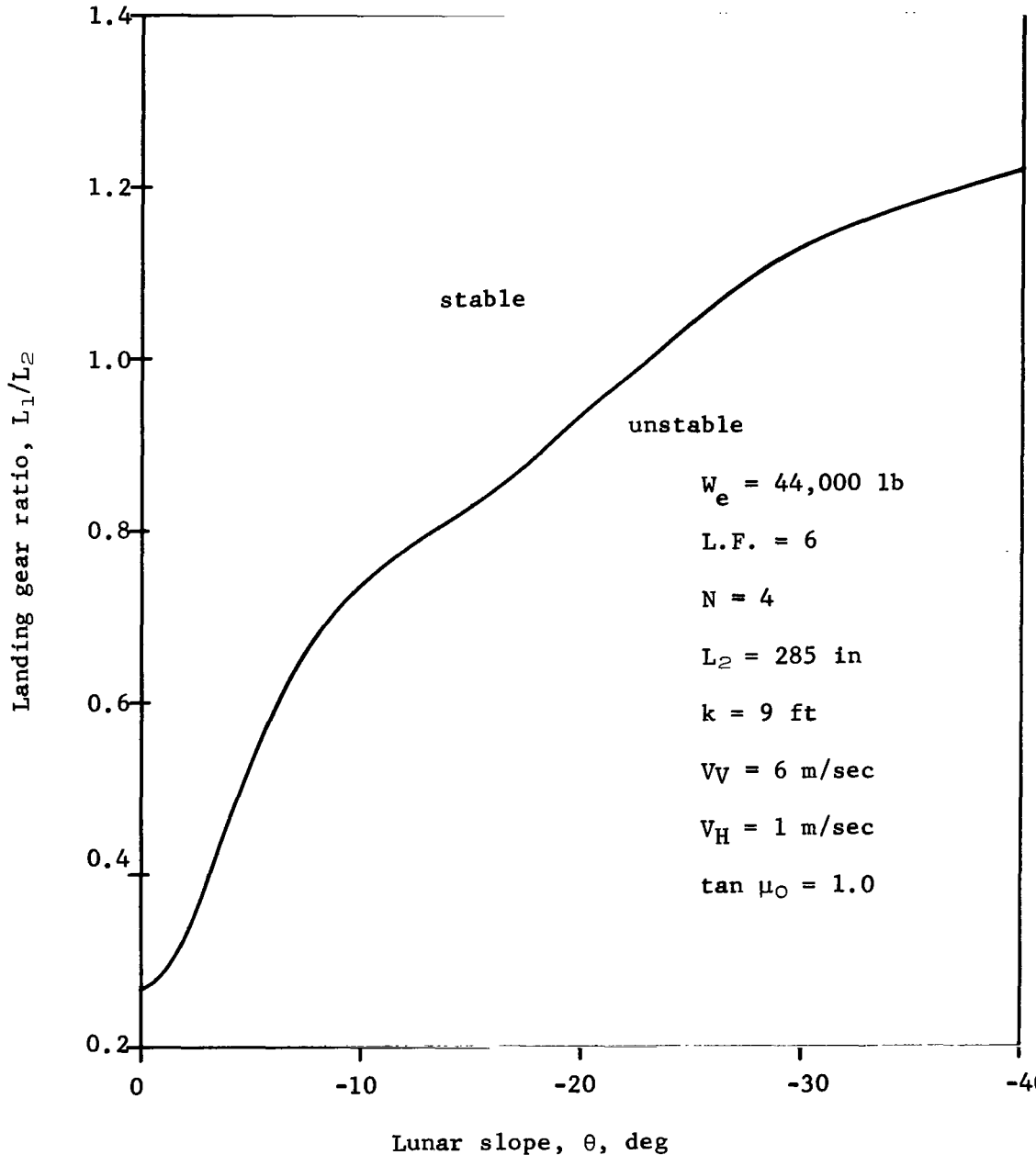

FIGURE 5. LANDING GEAR RATIO AS A FUNCTION OF LUNAR SLOPE

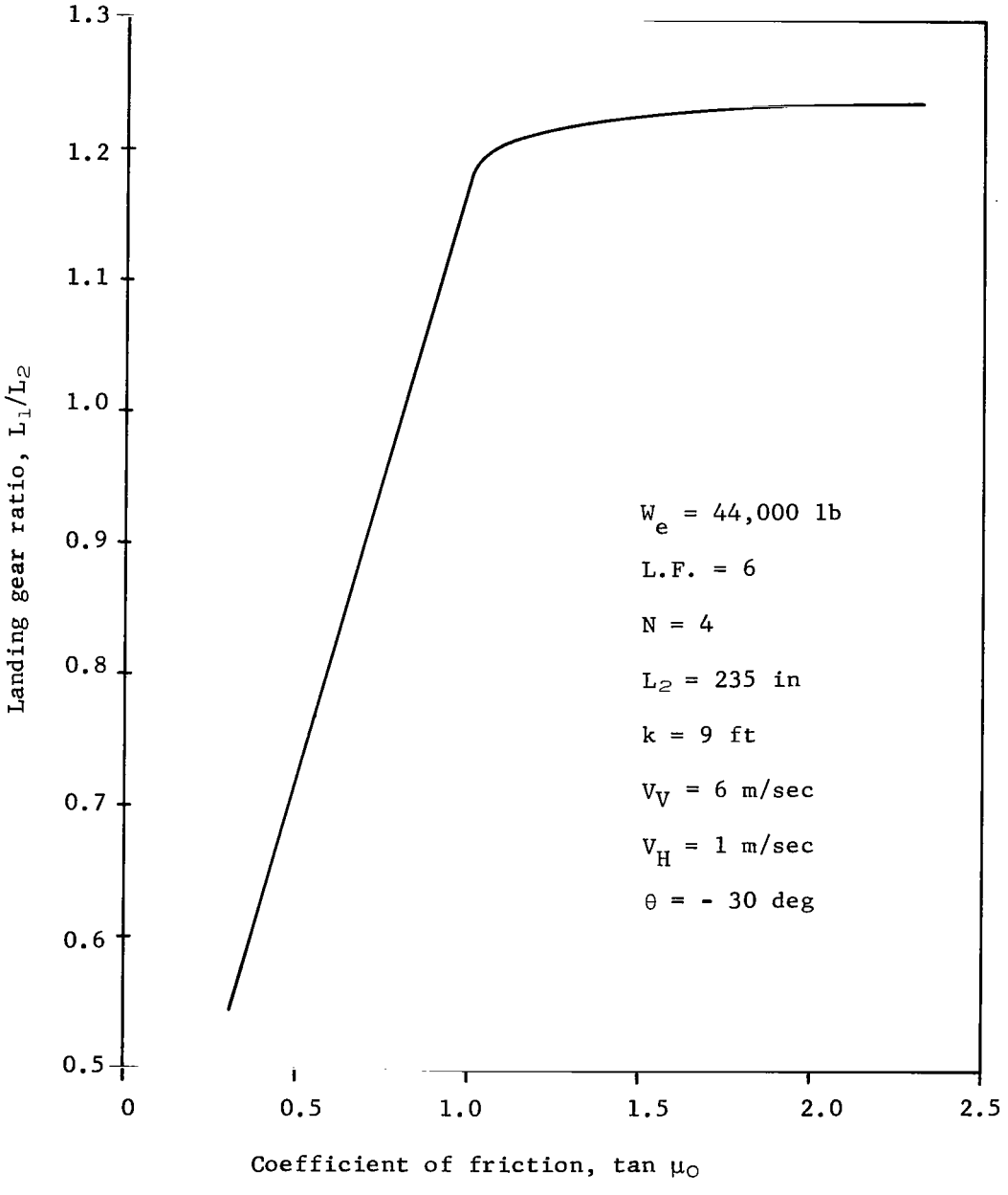

FIGURE 6. LANDING GEAR RATIO AS A FUNCTION OF THE COEFFICIENT OF FRICTION

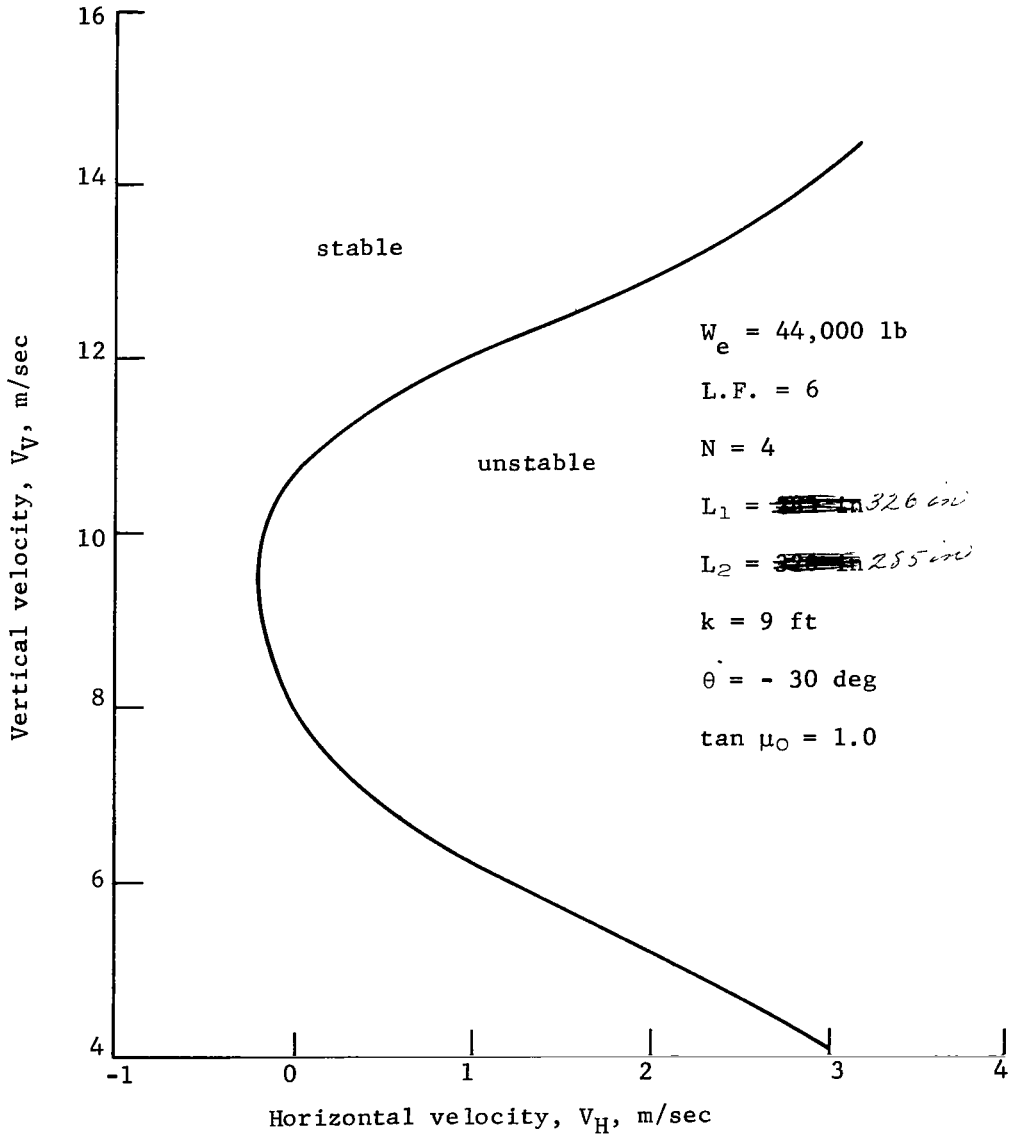

FIGURE 7. DOWNHILL STABILITY BOUNDARY AS A FUNCTION OF TOUCHDOWN VELOCITY

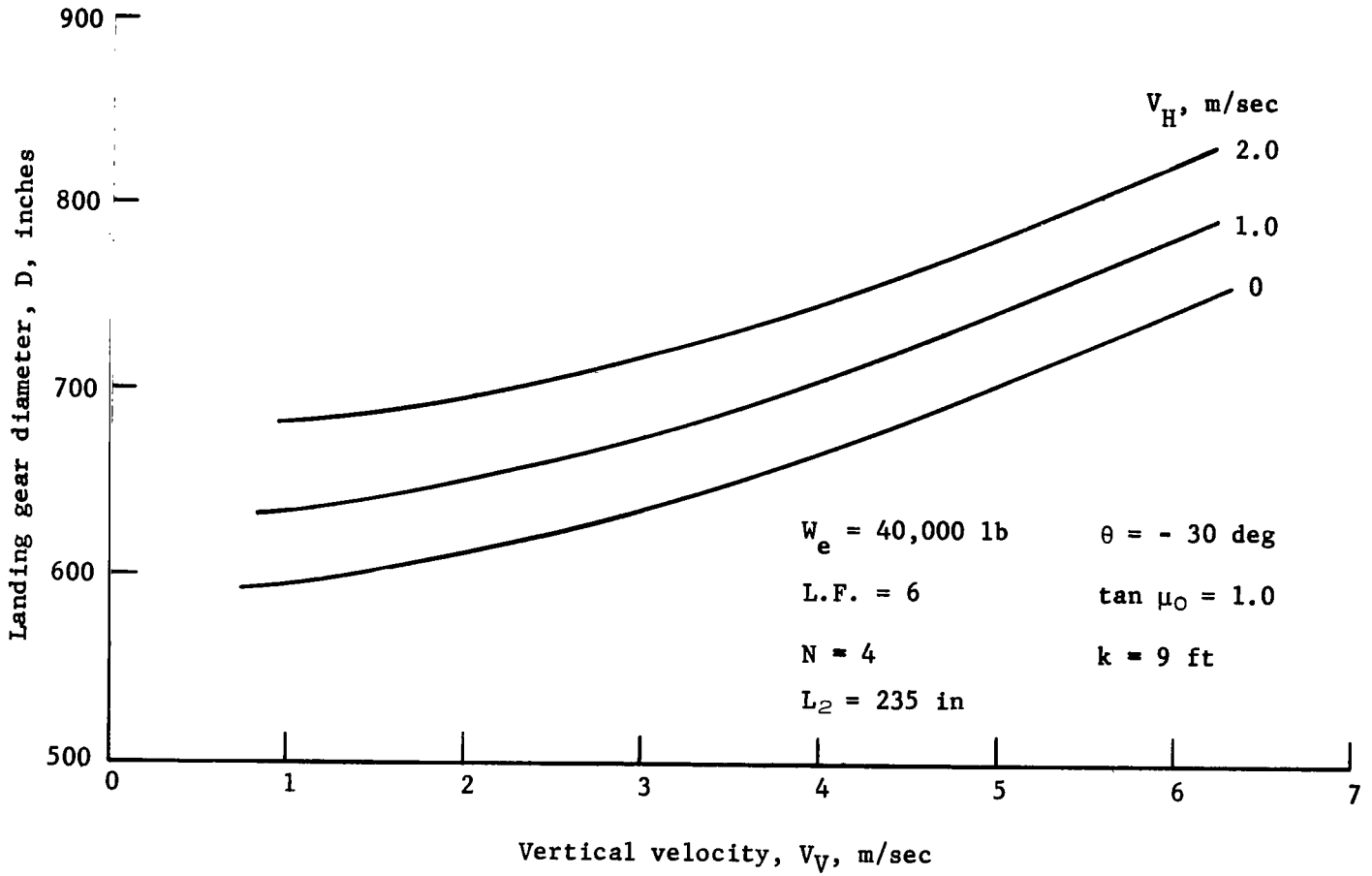

FIGURE 8. LANDING GEAR DIAMETER AS A FUNCTION OF TOUCHDOWN VELOCITY

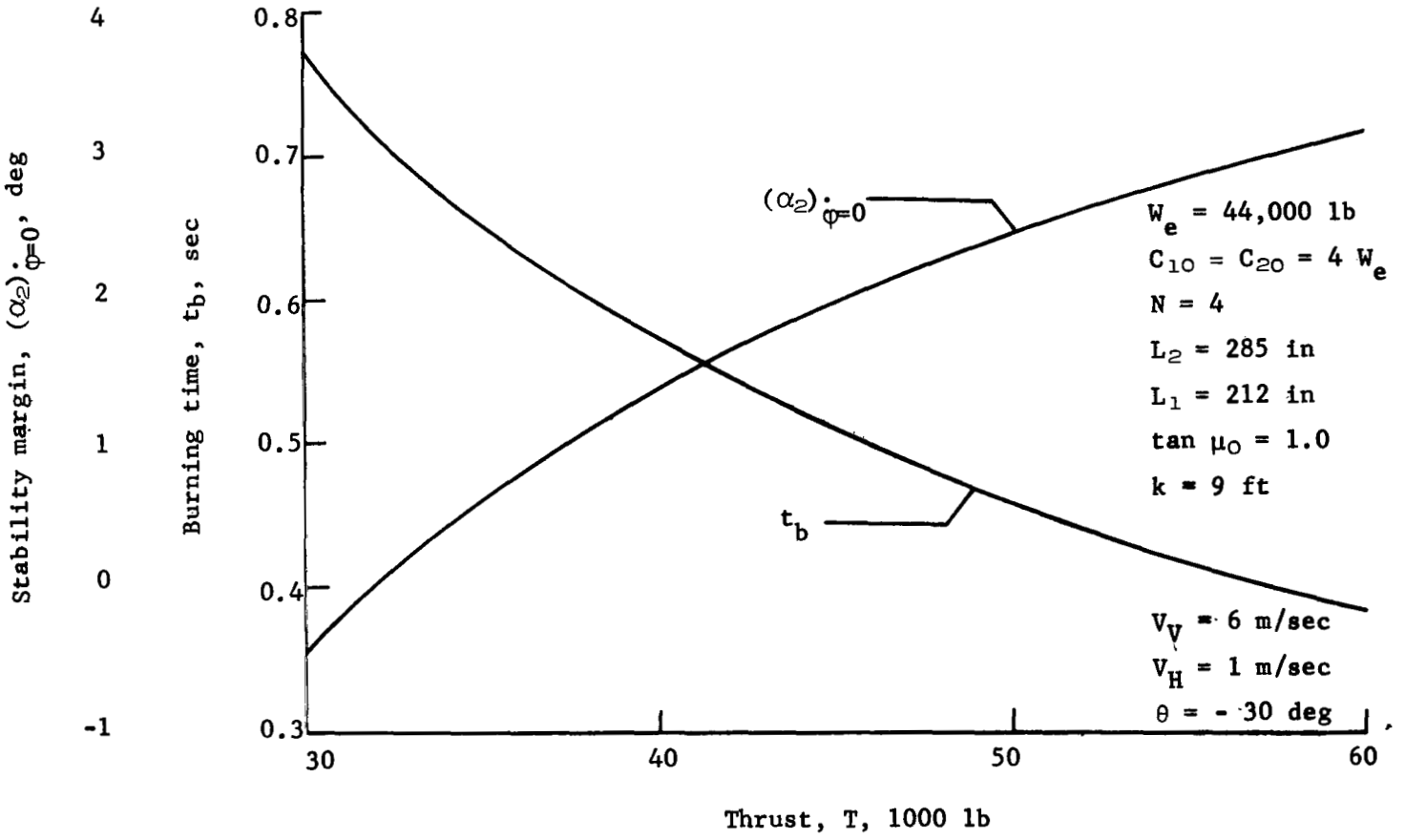

FIGURE 9. TOUCHDOWN DYNAMICS RESULTS WITH STABILIZATION ROCKET

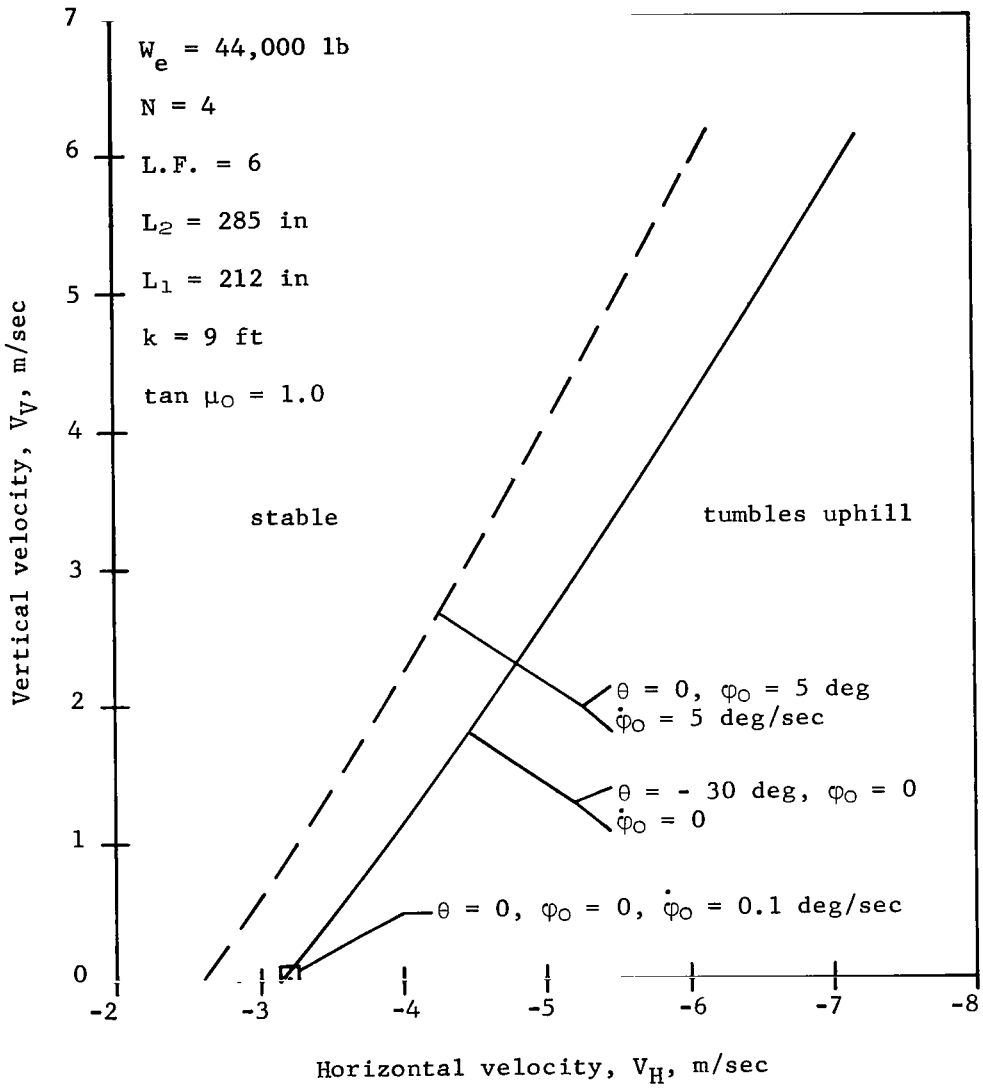

FIGURE 10. UPHILL STABILITY BOUNDARY AS A FUNCTION OF TOUCHDOWN VELOCITY

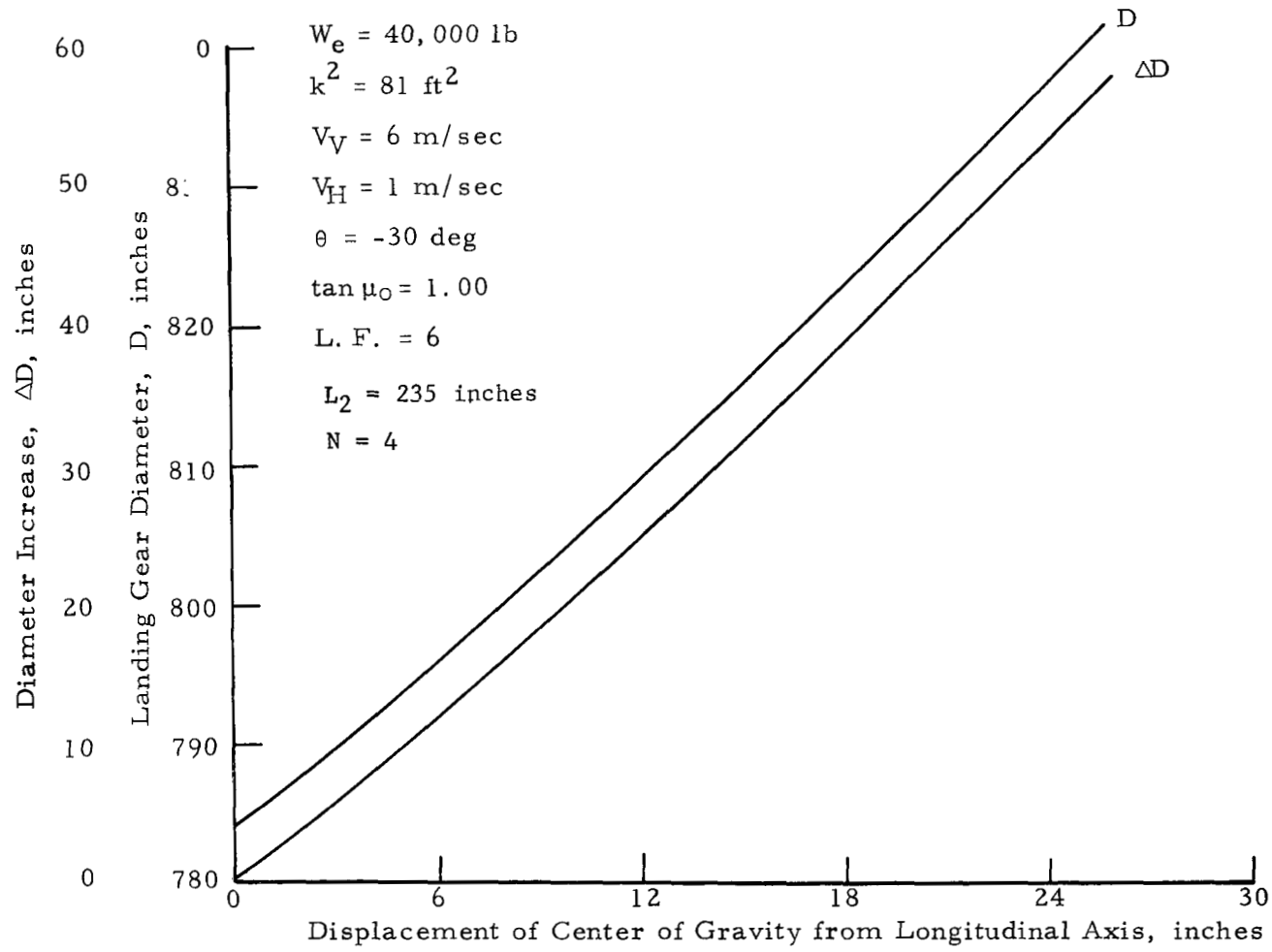

FIGURE 11. EFFECT OF CENTER OF GRAVITY SHIFT FROM LONGITUDINAL AXIS ON LANDING GEAR DIAMETER

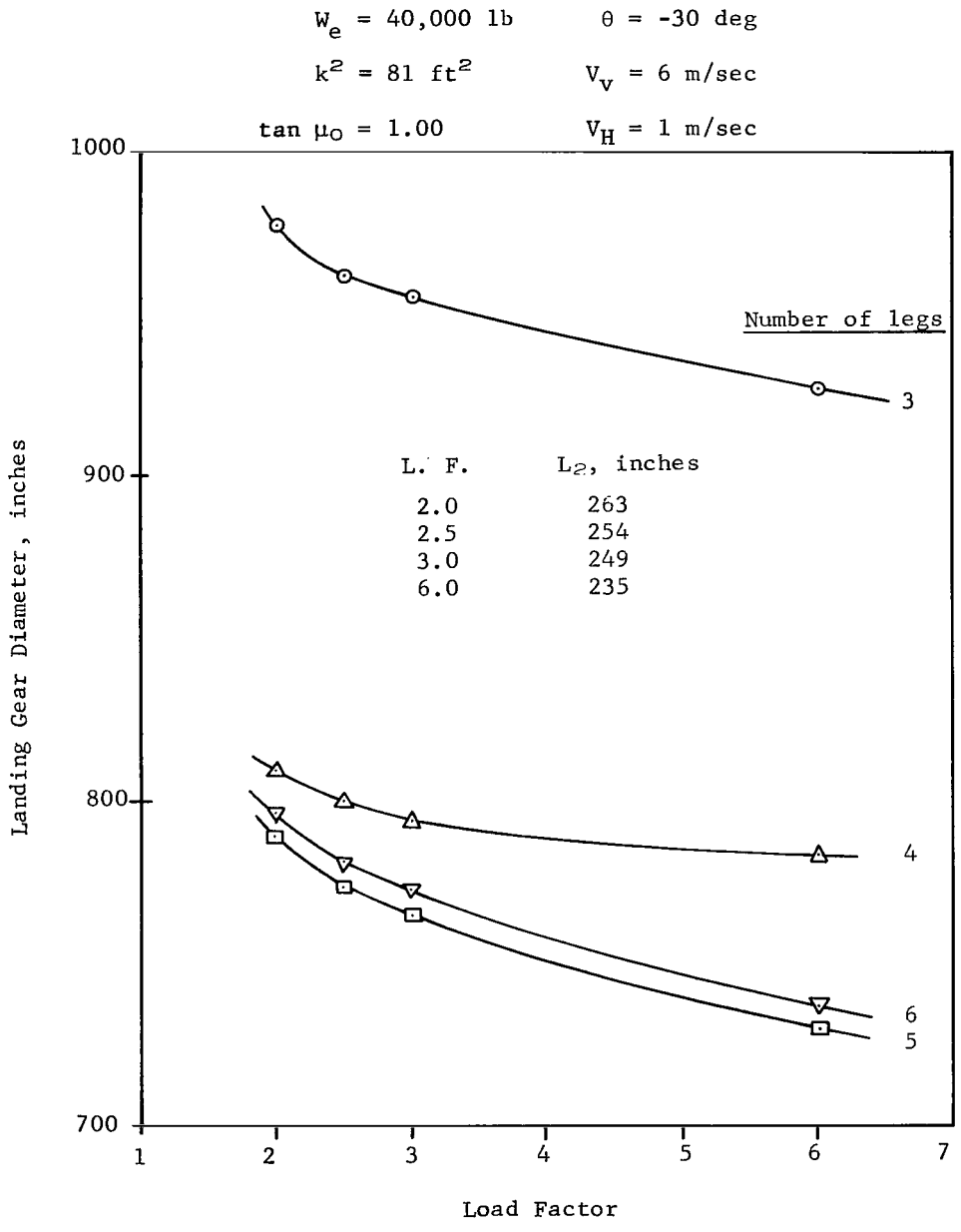

FIGURE 12. EFFECT OF LOAD FACTOR AND NUMBER OF LEGS ON LANDING GEAR DIAMETER

W_e = 40,000 lb

k^2 = 81 ft^2

tan μ_o = 1.0

θ = - 30 deg

V_V = 6 m/sec

V_H = 1 m/sec

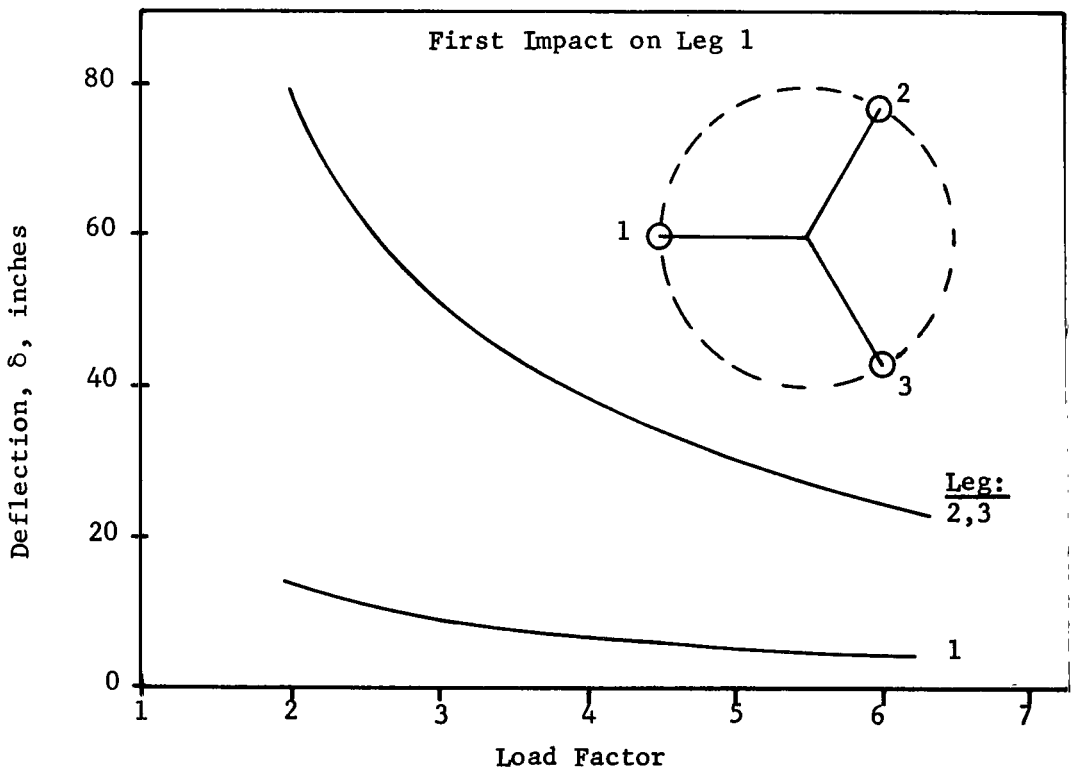

FIGURE 13. LEG DEFLECTION FOR THREE-LEGGED VEHICLE

W_e = 40,000 lb θ = -30 deg

k^2 = 81 ft^2 V_V = 6 m/sec

tan μ_o = 1.00 V_H = 1 m/sec

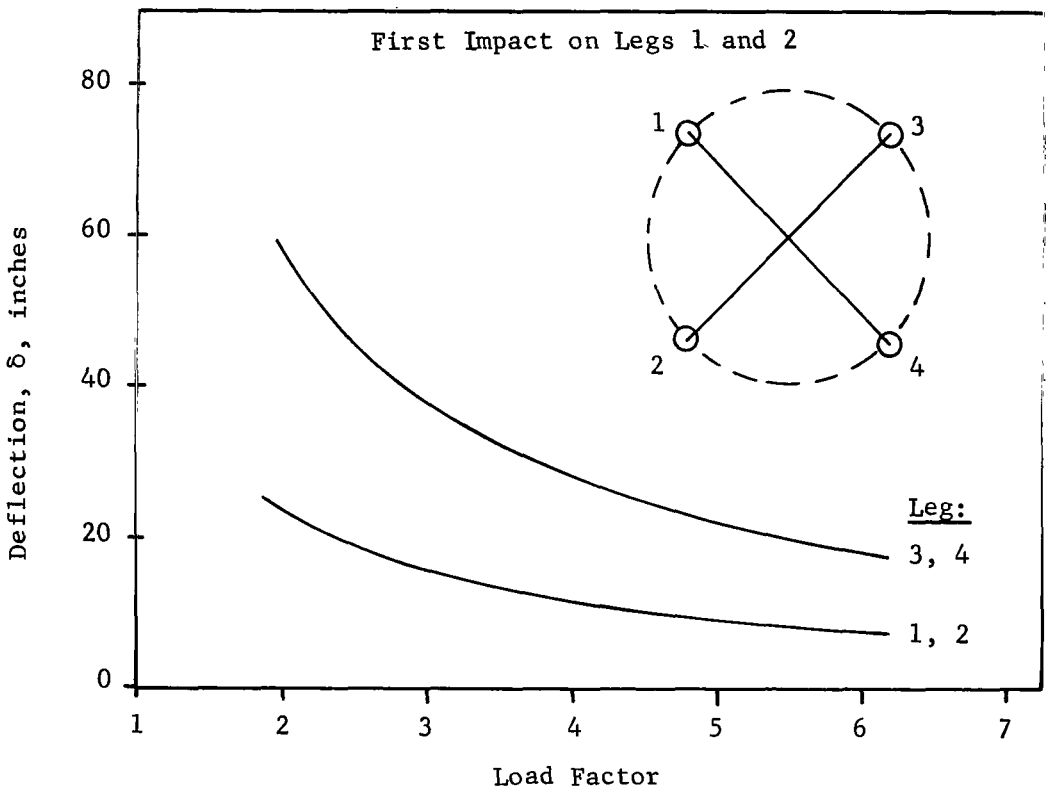

FIGURE 14. LEG DEFLECTION FOR FOUR-LEGGED VEHICLE

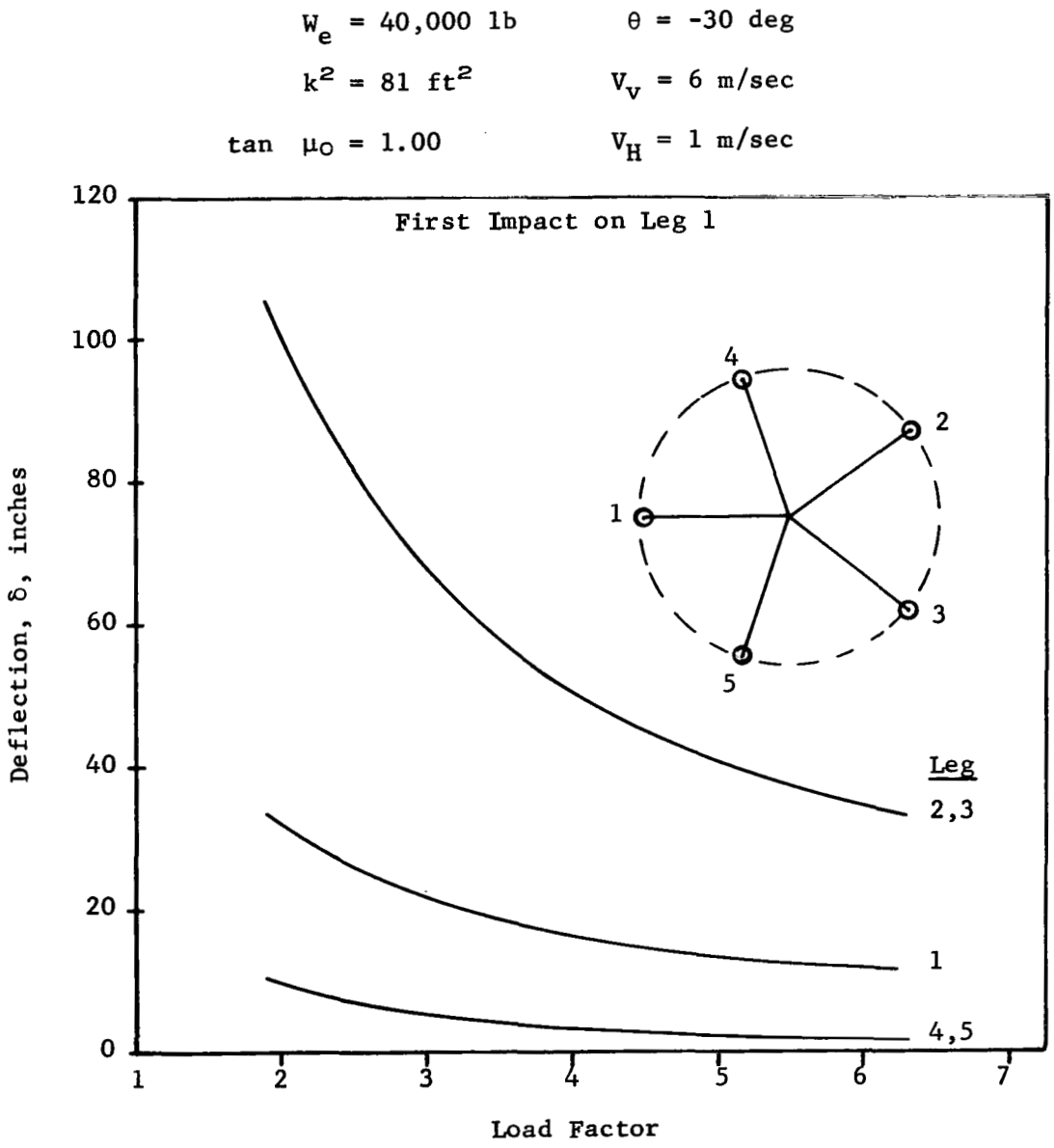

FIGURE 15. LEG DEFLECTION FOR FIVE-LEGGED VEHICLE

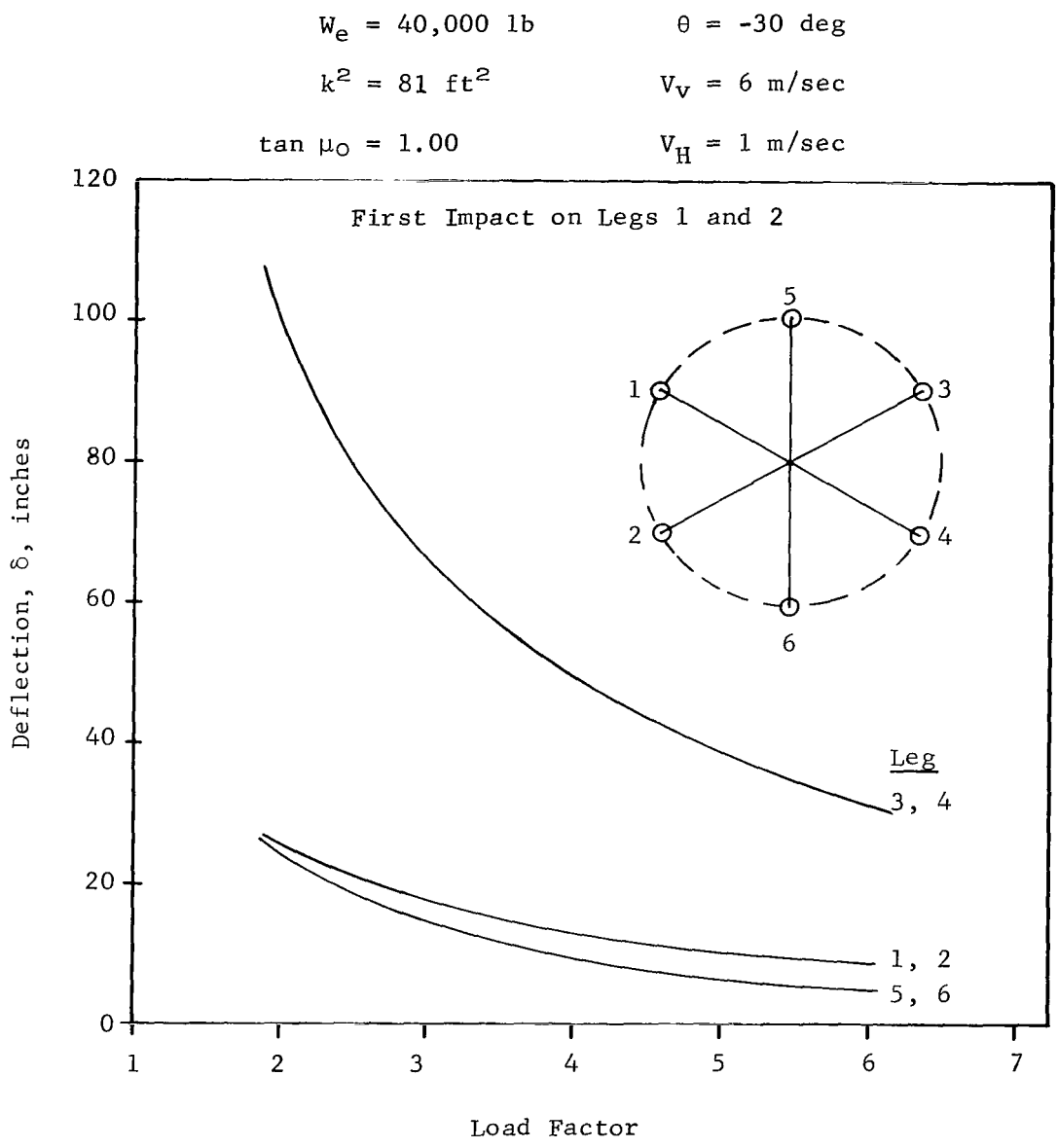

FIGURE 16. LEG DEFLECTION FOR SIX-LEGGED VEHICLE

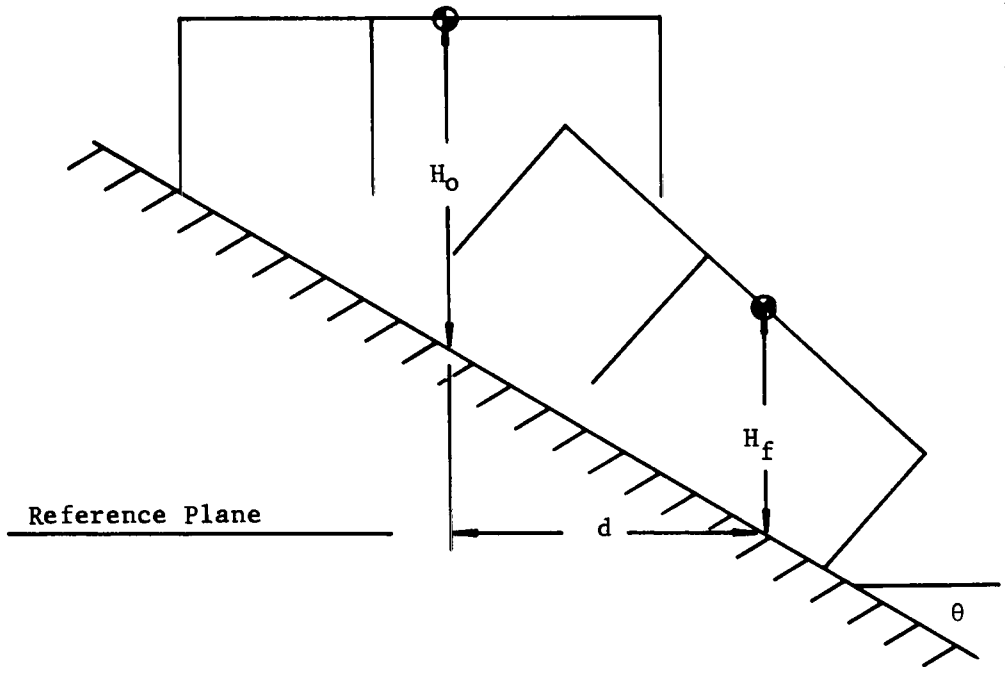

N = 5

L.F. = 6

D = 733 in

W_e = 40,000 lb

k = 9 ft

L_2 = 235 in

V_V = 6 m/sec

V_H = 1 m/sec

θ = 30 deg

tan μ_o = 1.0

FIGURE 17. INITIAL AND FINAL POSITIONS OF VEHICLE